Asian Journal of Chemistry; Vol. 32, No. 11 (2020), 2753-2762

ASIAN JOURNAL OF CHEMISTRY

https://doi.org/10.14233/ajchem.2020.22821

Design, Synthesis and Antimicrobial Evaluation of Novel 2-Thiobenzimidazole Derivatives: *in silico* and *in vitro* Approach

C. NARESH BABU[1], S. TRIVENI[2,*], M. VIJAYA JYOTHI[2], B. YAMUNA[2] and A. YAMINI[2]

[1]Molecular Modeling and Drug Discovery Division, RERDS-CPR, Raghavendra Institute of Pharmaceutical Education and Research (RIPER)-Autonomous, K.R. Palli Cross, Near SK University, Anantapur-515721, India
[2]Department of Pharmaceutical Chemistry, Raghavendra Institute of Pharmaceutical Education and Research (RIPER)-Autonomous, K.R. Palli Cross, Near SK University, Anantapur-515721, India

*Corresponding author: Email: s.trivenipharma@gmail.com

Received: 8 May 2020; *Accepted*: 4 July 2020; *Published online*: 28 October 2020; AJC-20098

The development of potent antimicrobial agents is more essential due to resistance developed in microorganisms towards the existing drugs. The diversity in the biological retort profile of benzimidazole more attracted the attention to develop novel compounds to its various potential against microorganisms. In present work, designed molecular structures docked against DNA gyrase subunit B and lanosterol 14α-demethylase (LAD) proteins. Interestingly, most of the compounds revealed excellent docking scores and interactions compared with the co-crystal ligands KKK, 1YN of LAD proteins 3LD6, 5V5Z than DNA gyrase subunit B proteins 5L3J and 4P8O. Then, the molecular properties were predicted by the Swiss ADME tool, the compounds showed no violation in Lipinski's rule and good synthetic accessibility. These compounds synthesized by stirring of 2-mercapto benzimidazole (**1**), epichlorohydrin (**2**) in the presence of sodium hydroxide gives 1-(1*H*-benzo[*d*]imidazole-2-ylthio)-3-chloropropan-2-ol (**3**), which upon refluxing with different substituted aliphatic and aromatic amines in methanol produces novel benzimidazole derivatives (**4a-l**). These compounds were characterized by their melting point, FT-IR, ^{1}H NMR and Mass spectral data. The synthesized molecules screened for antibacterial and antifungal activity. The compound **4l** exhibited excellent activity at MIC 0.4 µg/mL against *C. albicans*. Compounds **4c** and **4e** showed MIC at 3.12 µg/mL against *E. coli* and the compounds **4l** and **4J** exhibited MIC at 3.12 µg/mL against *S. aureus*. Docking studies and activity result reveals the novel benzimidazole compound **4l** has excellent antifungal and antibacterial effect.

Keywords: Benzimidazole, Swiss ADME, Molecular docking studies, Antibacterial activity, Antifungal activity.

INTRODUCTION

The emergence of resistance in various microbes due to mutations and severe toxic effects leads to dwindling digit of active antibiotic drugs in the treatment, it is a foremost issue for the discovery and development of newer efficient antimicrobials [1]. Benzimidazole is a bioactive, aromatic, nitrogen-containing heterocyclic scaffold *i.e.* imidazole ring fused with benzene ring [2]. In drug discovery, this benzimidazole heterocyclic scaffold has greater importance because of its very resilient application in the field of medicine [3]. From the literature , the drugs or compounds with different substitutions in benzimidazole pharmacophore divulges that are allied with a diverse kind of therapeutic activities like antimicrobial, anthelmintic, anticonvulsant, anti-inflammatory, antipsychotic, antioxidant, antihistaminic, antiviral, *etc*. [4,5]. This attracting the medicinal researchers to develop exciting molecules with high potential activity [6] by effective binding interactions in the protein active site with minimal toxicity [7].

To find the best kind of molecule, the designed library docked against with DNA gyrase subunit B protein of *Escherichia coli* (5L3J) and *Staphylococcus aureus* (4P8O) to predict bacterial inhibitory nature by their interactions and docking score comparing with co-crystal ligands in the proteins. The bacterial DNA gyrase subunit B is a validated target for the discovery of antibacterial drugs, it controls replication of bacterial DNA in its topological state [8]. A benzothiazole inhibitor 6G9 is present as a co-crystal in DNA gyrase subunit B of *E. coli* [8] and an aminobenzimidazole urea inhibitor 883 is present as a co-crystal ligand in DNA gyrase subunit B

of *S. aureus* [9]. The ligands (6G9 and 883 inhibitors) benzothiazole and benzimidazole pharmacophore in both proteins 5L3J and 4P8O does not make any interactions at the active site. The substitutions to these pharmacophores only making interactions with amino acids at the active site. Similarly, to know the antifungal nature of the designed library docked against human lanosterol 14α-demethylase (CYP51) in complex with ketoconazole -KKK (3LD6) protein and crystal structure of CYP51 from the pathogen *Candida albicans* in complex with itraconazole-1YN (5V5Z) protein [10,11]. The fungal activity is predicted by comparing interactions and docking scores of the generated library with the standard azole co-crystals KKK and 1YN of these lanosterol 14α-demethylase proteins. Further *in silico* ADME studies by Swiss ADME online software tool [12] helps to identify the pilot molecule from the library by predicting different parameters like iLogP [13], hydrogen bond acceptors (HBA), hydrogen bond donors (HBD), rotational bonds (RB), topological polar surface area (TPSA), molar refractivity (MR), solubility (LogS), skin permeability (LogKp), GI absorption, BBB permeation [14], cytochrome p450 (1A2, 2C19, 2C9, 2D6 and 3A4) inhibition, leadlike ness, synthetic accessibility, violation in Lipinski's rule of 5, PAINS, Ghose, Muegge filter, *etc*. This early assessment of molecular docking and ADME studies of the compounds drastically reduces the failure in clinical trial phases. In present work, we represented the synthesis of novel thiobenzimidazole derivatives initially by the synthesis of 1-(1*H*-benzo[*d*]imidazole-2-ylthio)-3-chloropropan-2-ol (**3**) by the reaction of 2-mercaptobenzimidazole (**1**), epichlorohydrin (**2**). Compound **3** further refluxed with different aliphatic and aromatic amines to get titled compounds of thiobenzimidazole derivatives (**4a-l**). The minimum inhibitory concentration (MIC) by serial dilution method [15,16] was used to know the antimicrobial activity of the synthesized compounds. For this screening study, *E. coli* (Gram-negative bacteria) and *S. aureus* (Gram-positive bacteria) were selected for *in vitro* antibacterial activity and for antifungal *Candida albicans* was selected. These activity data compared with the standard MIC values of ciprofloxacin and ketoconazole.

EXPERIMENTAL

Melting points were determined in open capillary tube using melting point apparatus and uncorrected. Thin-layer chromatography was performed on pre-coated silica gel strips and spots were visualized by iodine vapours. Infrared spectra (ν, cm^{-1}) were recorded on a FT-IR 4000; using KBr disks. Mass spectra were obtained on the GC-Mass spectrometer at 70 eV using a direct insertion probe method. NMR spectra were taken on BRUKERAV400-400 MHz high-resolution multinuclear FT-NMR spectrometer using TMS as an internal standard. Calculation of molecular physio-chemical properties by Swiss ADME tool. Molecular docking studies by Schrodinger Glide software and evaluation of *in vitro* antimicrobial activity (MIC method) by serial dilution method.

Molecular docking studies: The generated structures of thiobenzimidazoles docking studies were analyzed by licensed Schrodinger Glide software version 2020_1.

Selection of proteins and preparation for docking: Novel thiobenzimidazoles were docked against DNA Gyrase subunit B of *Escherichia coli*, *Staphylococcus aureus* and lanosterol 14α-demethylase of human and *Candida albicans* to establish their biological efficacy towards bacteria and fungi. (i) *Escherichia coli* DNA gyrase B in complex with benzothiazole based inhibitor (5L3J) protein is a validated target in drug discovery of antimicrobials, it is mainly responsible to control the topological state of DNA during replication. This protein has chain A with 378 amino acid residues co-crystal ligand 2-[[2-[[4,5-*bis*(bromanyl)-1~{*H*}-pyrrol-2-yl]carbonylamino]-1,3-benzothiazol-6-yl]amino]-2-oxidanylidene-ethanoic acid (6G9) and iodide ion. (ii) *S. aureus* gyrase bound to an aminobenzimidazole urea inhibitor (4P8O) protein has potent aminobenzimidazole urea, it shows broad-spectrum antibacterial activity by inhibiting DNA gyrase B (GyrB). This protein contains unique chains of A and B with 187 amino acid residues and co-crystal 1-ethyl-3-[5-(5-fluoropyridin-3-yl)-7-(pyrimidin-2-yl)-1*H*-benzimidazol-2-yl]urea (883). In this protein, the water molecules with residue number 442 and 471 showing interactions with the 883 and protein. Hence these two water molecules also considered while protein preparation for docking. (iii) Crystal structure of human lanosterol 14α-demethylase (CYP51) in complex with ketoconazole (3LD6) protein, the hydrophobic binding of azole containing molecules mostly occurs with amino acid residues of active site. This prevents the biosynthesis of sterol by demethylation of the C-14 position of sterol precursors in eukaryotes, it is catalyzed by CYP51. This protein has unique chains A and B with 461 amino acid residues along with co-crystal ketoconazole (KKK). (iv) Structure of CYP51 from the pathogen *Candida albicans* (5V5Z) protein has Itraconazole as co-crystal, it is an azole containing drug targeting mainly lanosterol 14α-demethylase (LDM). This protein contains chain A with 537 amino acid residues along with Protoporphyrin IX Containing Fe (CYP51) and itraconazole (1YN).

These proteins were prepared for docking by downloading PDB format from protein data bank by allocating bond orders, the addition of hydrogens, the creation of zero-order bonds to metals, filling of missing atoms, side chains using prime and applying force field OPLS3 in the maestro protein preparation wizard. A grid is generated by selecting any one atom of the co-crystal structure in the protein, the generated grid X, Y and Z coordinates for the protein 5L3J is -12.3, 19.77 and 22.46, for the protein 4P8O, for the protein 3LD6 is 42.47, 4.96 and 2.04, for the protein 5V5Z is -36.96, -18.08 and 26.76.

Ligand preparation: The structures of thiobenzimidazoles were drawn in Chemdraw Ultra 8.0.3 and saved as MDL Molfiles, these Molfiles converted to structure data file (SDF) format in OpenBabel GUI (Chris Morley). These SDF formats of the molecules were imported into maestro workspace and energy minimized by the OPLS3 force field in ligprep from the tasks menu.

Virtual docking: Glide ligand docking utilized for docking of all molecules to the above-mentioned proteins along with their co-crystal ligand.

***in silico* ADME studies by SwissADME:** A drug will be potent when it reaches its active target in the body at sufficient

amount and produces biological effect in its active form. As per new scenario, *in silico* prediction is a valid alternate to experimental studies and plays a major role in selection of hit molecules from large library in drug discovery process. The Swiss ADME web tool gave a very easy input either by drawing the structure or by giving SMILES notation of the structures, this tool predicted various properties related to physico-chemical, pharmacokinetics, drug-likeness and synthetic accessibility *etc*. At a time a large number of structures are predicted to diverse properties and helps in selection of which compounds to synthesize, test for further *in vitro* and *in vivo* studies to produce best efficacious drug for the treatment of patients with less toxic effects. By this early assessment drastically decreases the pharmacokinetic relevant failure during clinical phase studies.

General procedure

Synthesis of 1-(1*H*-benzo[*d*]imidazole-2-ylthio)-3-chloropropan-2-ol (3): To a mixture of mercaptobenzimidazole (**1**) (0.01 mol) and epichlorohydrin (**2**) (0.01 mol) and aqueous sodium hydroxide solution (10%, 5 mL) was added dropwise with constant stirring for 1 h. Then the solution was cooled to room temperature. The completion of the reaction was determined by thin-layer chromatography using ethyl acetate: *n*-hexane (7:3) as the mobile phase and spots were visualized by iodine vapours.

1-(1*H*-Benzo[*d*]imidazole-2-ylthio)-3-chloropropan-2-ol (3): Compound **3**, $C_{10}H_{11}N_2OSCl$, Yield 82%, R_f value 0.78, m.p. 162-164 ºC, IR (KBr, ν_{max}, cm^{-1}): 3645.88 (O-H *str.*), 2922.40 (C-H *str.*, -CH_2-), 1305.24 (C-N *str.*, 2º amine), 1356.58 (C-N *str.*, 3º amine), 1108.60 (C-O *str.* 2º OH), 732.25 (C-Cl *str.*), 790.44 (C-S *str.*), 1462.72 (C-H deformation, -CH_2-); ^{1}H NMR (400 MHz, DMSO) δ ppm: 2.05 (s, 1H, -OH), 2.90-3.65 (m, 4H, -CH_2-), 3.92 (m, 1H, -CH-), 5.05 (s, 1H, -NH), 7.46-7.82 (d, t, 4H, aromatic).

Synthesis of 2-thiobenzimidazole derivatives (4a-l): An equimolar mixture of 1-(1*H*-benzo[*d*]imidazole-2-ylthio)-3-chloropropan-2-ol (**3**) and different substituted aromatic and aliphatic amine were dissolved in methanol and this mixture refluxed for 2 h at 80 ºC. The reaction mixture was poured into a crushed ice to induce crystallization. The completion of the reaction was determined by thin-layer chromatography using ethyl acetate:toluene (6:4) as the mobile phase and spots visualized by iodine vapours (**Scheme-I**).

1-((1*H*-Benzo[*d*]imidazol-2-yl)thio)-3-(ethylamino)-propan-2-ol (4a): Compound **4a**, $C_{12}H_{17}N_3OS$, Yield 66%, R_f value 0.64, m.p. 196-198 ºC, molecular ion peak at *m/z* 251.40; IR (KBr, ν_{max}, cm^{-1}): 3598.20 (O-H *str.*), 3350.86 (N-H *str.*, dialkyl), 2910.52 (C-H *str.*, -CH_2-), 1290.66 (C-N *str.*, 2º amine), 1345.17 (C-N *str.*, 3º amine), 1100.24 (C-O *str.* 2º OH), 784.29 (C-S *str.*), 2964.81 (C-H *str.*, -CH_3); ^{1}H NMR (400 MHz, DMSO) δ ppm: 1.12 (t, 3H, -CH_3), 1.95 (s, 1H, -NH), 2.65-3.38 (m, 6H, -CH_2-), 3.55 (s, 1H, -OH), 5.08 (s, 1H, -NH), 7.25-7.68 (d, t, 4H, aromatic).

1-((1*H*-Benzo[*d*]imidazol-2-yl)thio)-3-hydrazinylpropan-2-ol (4b): Compound **4b**, $C_{10}H_{14}N_4OS$, Yield 76%, R_f value 0.82, m.p. 206-208 °C, molecular ion peak at *m/z* 238.13;

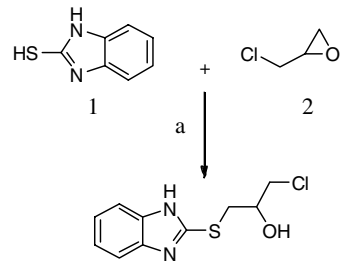

1-(1*H*-benzo[*d*]imidazol-2-ylthio)-3-chloropropan-2-ol (**3**)

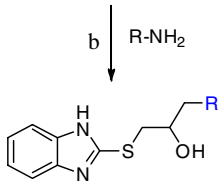

1-(1*H*-benzo[*d*]imidazol-2-ylthio)-3-substituted propan-2-ol (**4a-l**)

Reagents and conditions (a) stirred 60 min, 10% NaOH (b) refluxed 2 h, methanol; **R** = **4a**. -NH-C_2H_5; **4b**. -NH-NH_2; **4c**. -NH-NH-C_6H_5; **4d**. -NH-C_6H_4-SO_2OH; **4e**. -NH-C_6H_4-*o*-NH_2; **4f**. -NH-C_6H_5; **4g**. -N-$(C_2H_5)_2$; **4h**. -NH-CH_2-C_6H_5; **4i**. –NH-CH (CH_3)$CH_2CH_2CH_3$; **4j**. –NH-C_6H_4-*m*-NO_2; **4k**. –NH-C_6H_4-*p*-OCH_3; **4l**. –NH-C_6H_4-*p*-CF_3

Scheme-I

IR (KBr, ν_{max}, cm^{-1}): 3622.80 (O-H *str.*), 2923.40 (C-H *str.*, -CH_2-), 1300.19 (C-N *str.*, 2º amine), 3390.42, 3332.24 (N-H *str.*, -NH_2), 1352.70 (C-N *str.*, 3º amine), 1098.52 (C-O *str.* 2° OH), 780.50 (C-S *str.*); ^{1}H NMR (400 MHz, DMSO) δ ppm: 2.00 (s, 3H, -NH and –NH_2), 2.67-3.25 (m, 4H, -CH_2-), 3.58 (s, 1H, -OH), 3.80 (m, 1H, -CH<), 5.04 (s, 1H, -NH), 7.20-7.62 (d, t, 4H, aromatic).

1-((1*H*-Benzo[*d*]imidazol-2-yl)thio)-3-(2-phenylhydrazinyl)propan-2-ol (4c): Compound **4c**, $C_{16}H_{18}N_4OS$, Yield 86%, R_f value 0.79, m.p. 225-227 ºC, molecular ion peak at *m/z* 314.60; IR (KBr, ν_{max}, cm^{-1}): 3648.11 (O-H *str.*), 2935.61 (C-H *str.*, -CH_2-), 1290.00 (C-N *str.*, 2º amine), 1350.69 (C-N *str.*, 3° amine), 1099.04 (C-O *str.* 2º OH), 794.23 (C-S *str.*); ^{1}H NMR (400 MHz, DMSO) δ ppm: 2.10, 4.02 (s, 1H, -NH), 2.52-3.31 (m, 4H, -CH_2-), 3.62 (s, 1H, -OH), 3.75 (m, 1H, -CH<), 5.02 (s, 1H, -NH of imidazole), 6.95-7.70 (d, t, 9H, aromatic).

4-((3-((1*H*-Benzo[*d*]imidazol-2-yl)thio)-2-hydroxypropyl)amino)benzenesulfonic acid (4d): Compound **4d**, $C_{16}H_{17}N_3O_4S_2$, Yield 70%, R_f value 0.66, m.p. 256-258 ºC, molecular ion peak at *m/z* 379.48; IR (KBr, ν_{max}, cm^{-1}): 1340.24 (S=O *str.*), 1150.11 (O-H *str.*, sulphonic acid), 3605.52 (O-H *str.*, 2º alcohol), 2915.93 (C-H *str.*, -CH_2-), 1288.75 (C-N *str.*, 2° amine), 1346.64 (C-N *str.*, 3º amine), 1100.01 (C-O *str.* 2° OH), 797.08 (C-S *str.*); ^{1}H NMR (400 MHz, DMSO) δ ppm: 2.04 (s, 1H, -SO_2OH), 2.95-3.40 (m, 4H, -CH_2-), 3.60 (s, 1H, 2°-OH), 3.78 (m, 1H, -CH=), 4.04 (s, 1H, -NH), 4.95 (s, 1H, -NH of imidazole), 7.25-7.62 (d, t, 4H, aromatic).

1-((1*H*-Benzo[*d*]imidazol-2-yl)thio)-3-((2-aminophenyl)-amino)propan-2-ol (4e): Compound **4e**, $C_{16}H_{18}N_4OS$, Yield 58%, R_f value 0.80, m.p. 210-212 °C, molecular ion peak at *m/z* 314.80; IR (KBr, ν_{max}, cm^{-1}): 3596.90 (O-H *str.*), 2922.10 (C-H *str.*, -CH_2-), 3504.54, 3410.23 (N-H *str.*, aromatic 1° amine), 1283.26 (C-N *str.*, 2° amine), 3450.24 (N-H, arlyalkyl), 1344.58 (C-N *str.*, 3° amine), 1101.54 (C-O *str.* 2° OH), 791.99

(C-S *str.*); ^{1}H NMR (400 MHz, DMSO) δ ppm: 3.98 (s, 1H, -NH), 2.98-3.40 (m, 4H, -CH_2-), 3.56 (s, 1H, -OH), 3.78 (m, 1H, -CH<), 5.00 (s, 1H, -NH of imidazole), 6.25 (s, 2H, -NH_2), 6.58-7.65 (d, t, 8H, aromatic).

1-((1*H*-Benzo[*d*]imidazol-2-yl)thio)-3-(phenylamino)-propan-2-ol (4f): Compound **4f**, $C_{16}H_{17}N_3OS$, Yield 75%, R_f value 0.83, m.p. 184-186 ºC, molecular ion peak at *m/z* 299.41; IR (KBr, ν_{max}, cm^{-1}): 3601.79 (O-H *str.*), 2916.11 (C-H *str.*, -CH_2-), 1297.19 (C-N *str.*, 2º amine), 3449.84 (N-H *str.*, arylalkyl), 1352.07 (C-N *str.*, 3º amine), 1100.22 (C-O *str.* 2º OH), 797.68 (C-S *str.*); ^{1}H NMR (400 MHz, DMSO) δ ppm: 2.84-3.25 (m, 4H, -CH_2-), 3.50 (s, 1H, -OH), 3.72 (m, 1H, -CH<), 4.12 (s, 1H, -NH), 4.90 (s, 1H, -NH of imidazole), 6.70-7.58 (d, t, 9H, aromatic).

1-((1*H*-Benzo[*d*]imidazol-2-yl)thio)-3-(diethylamino)-propan-2-ol (4g): Compound **4g**, $C_{14}H_{21}N_3OS$, Yield 55%, R_f value 0.60, m.p. 220-222 ºC, molecular ion peak at *m/z* 279.54; IR (KBr, ν_{max}, cm^{-1}): 3644.12 (O-H *str.*), 3328.70 (N-H *str.*, dialkyl), 2930.00 (C-H *str.*, -CH_2-), 1287.01 (C-N *str.*, 2º amine), 1351.28 (C-N *str.*, 3º amine), 1100.07 (C-O *str.* 2º OH), 797.11 (C-S *str.*), 2970.26 (C-H *str.*, -CH_3); ^{1}H NMR (400 MHz, DMSO) δ ppm: 1.25 (t, 6H, -CH_3), 2.35-3.21 (m, 8H, -CH_2-), 3.50 (s, 1H, -OH), 3.81 (m, 1H, -CH<), 5.12 (s, 1H, -NH), 7.20-7.62 (d, t, 4H, aromatic).

1-((1*H*-Benzo[*d*]imidazol-2-yl)thio)-3-(benzylamino)-propan-2-ol (4h): Compound **4h**, $C_{17}H_{19}N_3OS$, Yield 77%, R_f value 0.74, m.p. 205-206 ºC, molecular ion peak at *m/z* 313.30; IR (KBr, ν_{max}, cm^{-1}): 3655.00 (O-H *str.*, 2º alcohol), 2938.24 (C-H *str.*, -CH_2-), 1279.59 (C-N *str.*, 2º amine), 3330.25 (N-H *str.*, dialkyl), 1350.88 (C-N *str.*, 3º amine), 1098.62 (C-O *str.* 2º OH), 778.04 (C-S *str.*); ^{1}H NMR (400 MHz, DMSO) δ ppm: 2.08 (s, 1H, -NH), 2.55-3.30 (m, 4H, -CH_2-), 3.54 (s, 1H, -OH), 3.75 (m, 1H, -CH<), 3.85 (s, 2H, -CH_2), 5.02 (s, 1H, -NH of imidazole), 7.15-7.75 (d, t, 9H, aromatic).

1-((1*H*-Benzo[*d*]imidazol-2-yl)thio)-3-(pentan-2-ylamino)propan-2-ol (4i): Compound **4i**, $C_{15}H_{23}N_3OS$, Yield 62%, R_f value 0.71, m.p. 262-265 ºC, molecular ion peak at *m/z* 293.43; IR (KBr, ν_{max}, cm^{-1}): 3585.74 (O-H *str.*), 3351.02 (N-H *str.*, dialkyl), 2935.55 (C-H *str.*, -CH_2-), 1300.51 (C-N *str.*, 2º amine), 1346.08 (C-N *str.*, 3º amine), 1098.25 (C-O *str.* 2º OH), 780.29 (C-S *str.*), 2955.33 (C-H *str.*, -CH_3); ^{1}H NMR (400 MHz, DMSO) δ ppm: 0.95, 1.10 (t, d, 6H, -CH_3), 1.45-1.49 (m, 4H, -CH_2-), 2.04 (s, 1H, -NH), 2.55-3.30 (m, 5H, -CH_2- and –CH=), 3.51 (s, 1H, -OH), 3.75 (m, 1H, -CH<), 4.90 (s, 1H, -NH), 7.35-7.72 (d, t, 4H, aromatic).

1-((1*H*-Benzo[*d*]imidazol-2-yl)thio)-3-((3-nitrophenyl)-amino)propan-2-ol (4j): Compound **4j**, $C_{16}H_{16}N_4O_3S$, Yield 78%, R_f value 0.69, m.p. 235-236 ºC, molecular ion peak at *m/z* 344.51; IR (KBr, ν_{max}, cm^{-1}): 3594.44 (O-H *str.*), 2900.48 (C-H *str.*, -CH_2-), 1550.64 (C-NO_2 *str.*), 850.22 (C-N *str.*, Ar C-NO_2), 1302.59 (C-N *str.*, 2º amine), 3450.66 (N-H *str.*, arylalkyl), 1352.24 (C-N *str.*, 3º amine), 1096.86 (C-O *str.* 2º OH), 802.73 (C-S *str.*); ^{1}H NMR (400 MHz, DMSO) δ ppm: 2.95-3.38 (m, 4H, -CH_2-), 3.55 (s, 1H, -OH), 3.70 (m, 1H, -CH<), 4.02 (s, 1H, -NH), 5.12 (s, 1H, -NH of imidazole), 7.27-7.84 (d, t, 8H, aromatic).

1-((1*H*-Benzo[*d*]imidazol-2-yl)thio)-3-((4-methoxyphenyl)amino)propan-2-ol (4k): Compound **4k**, $C_{17}H_{19}N_3O_2S$, Yield 85%, R_f value 0.81, m.p. 222-224 ºC, molecular ion peak at *m/z* 329.22; IR (KBr, ν_{max}, cm^{-1}): 2825.42 (C-H *str.*, OCH_3), 3610.25 (O-H *str.*), 2940.49 (C-H *str.*, -CH_2-), 1306.11 (C-N *str.*, 2º amine), 3445.66 (N-H *str.*, arylalkyl), 1359.31 (C-N *str.*, 3º amine), 1097.69 (C-O *str.* 2° OH), 1458.67 (C-H deformation, -OCH_3), 781.23 (C-S *str.*); ^{1}H NMR (400 MHz, DMSO) δ ppm: 2.95-3.35 (m, 4H, -CH_2-), 3.57 (s, 1H, -OH), 3.74 (m, 1H, -CH<), 3.85 (s, 3H, -OCH_3), 4.06 (s, 1H, -NH), 5.04 (s, 1H, -NH of imidazole), 6.75 (d, 4H, aromatic), 7.31-7.63 (d, t, 4H, aromatic ring of benzimidazole)

1-((1*H*-Benzo[*d*]imidazol-2-yl)thio)-3-((4-(trifluoro-methyl)phenyl)amino)propan-2-ol (4l): Compound **4l**, $C_{17}H_{16}N_3OSF_3$, Yield 68%, R_f value 0.77, m.p. 197-199 °C, molecular ion peak at *m/z* 367.40; IR (KBr, ν_{max}, cm^{-1}): 3647.70 (O-H *str.*), 1254.68 (C-F *str.*), 2933.59 (C-H *str.*, -CH_2-), 1301.00 (C-N *str.*, 2º amine), 3452.29 (N-H *str.*, arylalkyl), 1343.71 (C-N *str.*, 3º amine), 1111.66 (C-O *str.* 2º OH), 800.28 (C-S *str.*); ^{1}H NMR (400 MHz, DMSO) δ ppm: 2.81-3.15 (m, 4H, -CH_2-), 3.42 (s, 1H, -OH), 3.68 (m, 1H, -CH<), 3.90 (s, 3H, -OCH_3), 4.12 (s, 1H, -NH), 4.88 (s, 1H, -NH of imidazole), 6.71-7.49 (d, t, 8H, aromatic).

Antimicrobial activity: *in vitro* Antimicrobial potency in MIC (µg/mL) of the synthesized thiobenzimidazoles were evaluated against *Staphylococcus aureus* (Gram-positive bacteria), *Escherichia coli* (Gram-negative bacteria), C*andida albicans* (fungal species). The growth of these microbes was regulated by using Brain Heart Infusion (BHI) broth, it is a nutritious, buffered culture medium autoclaved at 121 °C nearly for 15 min having the composition-infusion of calf brain, beef heart, protease peptone, dextrose, sodium chloride, disodium phosphate. The above-mentioned microorganisms 5 µL was taken from the stock cultures and mixed with 2 mL of BHI broth. By using serial dilution method final concentrations of each compound to evaluate for their antimicrobial activity. For each compound 10 tubes were taken, initially in one tube 20 µL of the compound was added and diluted with 380 µL of BHI broth. In the remaining 9 tubes added BHI broth (200 µL) separately for dilution. Then 200 µL was taken fom the first tube and added to the 2nd tube containing previously added 200 µL of BHI broth and gives 10^{-1} dilution. From 10^{-1} second tube, 200 µL solution was transferred to 3rd tube to get 10^{-2} dilution, likewise procedure is repeated (serial dilution) up to 10^{-9} dilution for all compounds and finally to get concentrations of 100, 50, 25, 12.5, 6.25, 3.12, 1.6, 0.8, 0.4 and 0.2 µg/mL. Finally 200 µL of prepared culture suspension added to serially diluted tubes and incubated for 24 h. The tubes were observed for turbidity formation and MIC of the compounds were recorded.

RESULTS AND DISCUSSION

Molecular docking: The compounds docking score and interactions with the DNA Gyrase subunit B proteins 5L3J and 4P8O by Glide ligan docking are shown in Table-1.

From virtual screening data of compounds with protein DNA gyrase subunit B of *E. coli* (5L3J), the compounds **4c**, **4e**, **4f** and **4b** showed better docking score -7.096, -6.935, -6.764 and -6.471 when related with docking score -6.423 of the co-crystal ligand of the protein 6G9 shown in Fig. 1. By

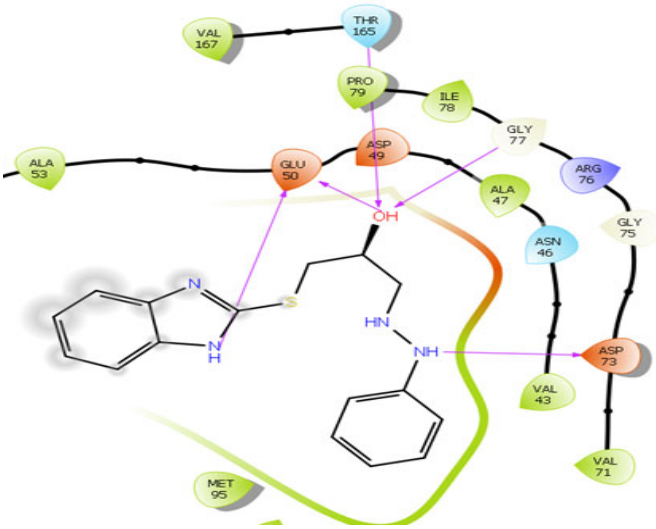

Compound **4c** (D.Score -7.096), H-bonding with GLU 50, ASP 73, GLY 77 and THR 165

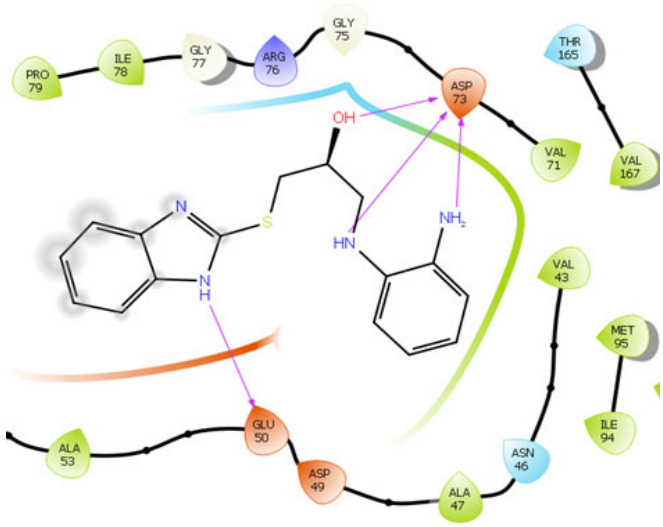

Compound **4e** (D.Score -6.935), H-bonding with GLU 50 and ASP 73

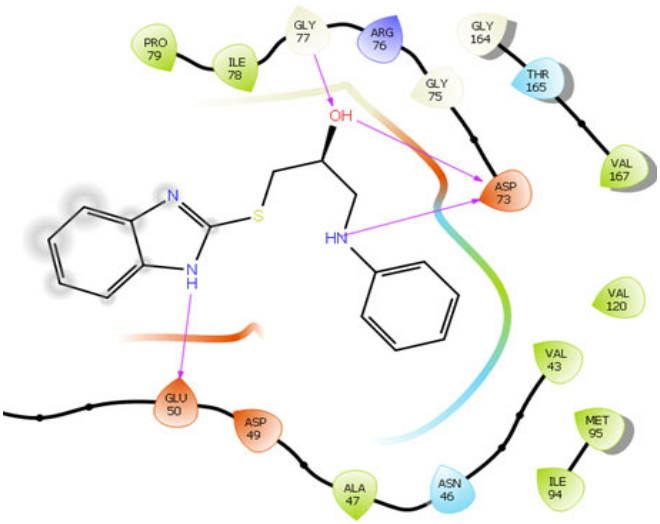

Compound **4f** (D.Score -6.764), H-bonding with GLU 50, ASP 73 and GLY 77

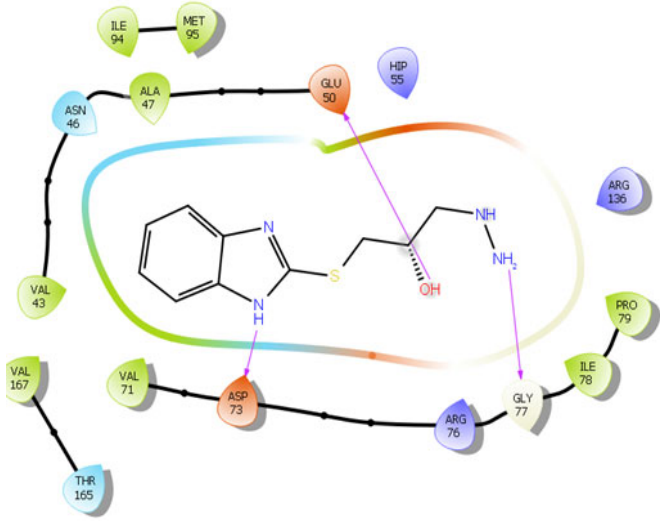

Compound **4b** (D.Score -6.471), H-bonding with GLU 50, ASP 73 and GLY 77

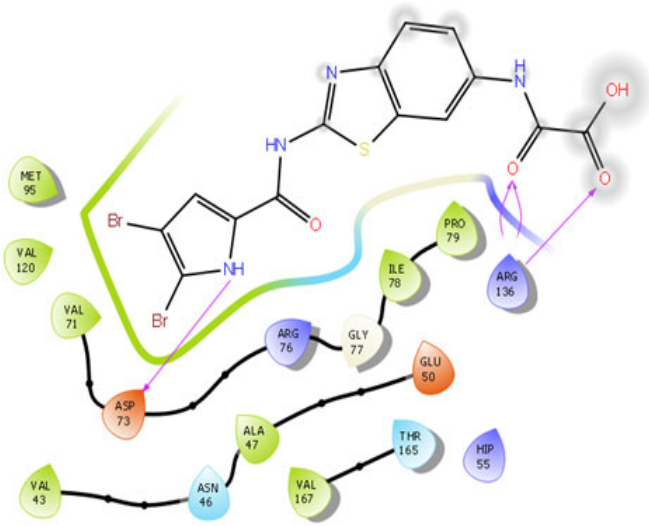

Co-crystal ligand - 6G9 (D.Score -6.423), H-bonding with ASP 73 and ARG 136

Fig. 1. 2D interactions of compounds and 6G9 ligand with amino acids of protein *E. coli* DNA Gyrase B (5L3J)

TABLE-1
DOCKING SCORE AND INTERACTIONS OF COMPOUNDS WITH DNA GYRASE SUBUNIT B

Compound code	*E. coli* DNA Gyrase B (5L3J)		*S. aureus* DNA Gyrase B (4P8O)	
	Docking score	Interactions	Docking score	Interactions
4a	-6.003	ASN 46, ASP 73	-6.155	GLU 58, ASP 81
4b	-6.471	GLU 50, ASP 73, GLY 77	-4.717	ASN 54, SER 55
4c	-7.096	GLU 50, ASP 73, GLY 77, THR 165	-4.166	GLU 58
4d	-6.264	ASN 46, GLU 50, ASP 73, VAL 120	-4.682	ASN 54, ASP 81, ARG 84
4e	-6.935	GLU 50, ASP 73	-5.067	ASN 54, ASP 57
4f	-6.764	GLU 50, ASP 73, GLY 77	-4.191	GLU 58
4g	-5.913	GLU 50, ASP 73	-3.933	GLU 58
4h	-5.192	ASP 73	-3.945	GLU 58
4i	-4.119	ASN 46, ASP 73	-2.362	GLU 58, GLY 85
4j	-6.332	ASN 46, ASP 73, VAL 120	-5.172	ASN 54, ARG 84, ARG 144
4k	-5.561	GLU 50, ASP 73, GLY 77	-4.041	GLU 58
4l	-5.564	ASP 73	-4.772	ASP 81
Co-crystal	-6.423 (6G9)	ASP 73, ARG 136	-6.938 (883)	ASP 81, ARG 144

observing the interactions of the 6G9 ligand active site, it indicated that the benzothiazole pharmacophore does not make any interactions with the protein, only the substituents pyrrole ring 2° amine-NH-, carbonyl and carboxylic groups represented H-bonding interactions with ASP 73 and ARG 136 of the protein. But, the benzimidazole pharmacophore 2º amine (-NH-), 2º alcohol and 1º and 2º amino groups of the substitutions of the compounds **4c**, **4e**, **4f** and **4b** makes greater H-bondings with amono acids of active site ASN 46, ASP 73, GLU 50, GLY 77, THR 165 and VAL 120. Among the library, the compounds substituted with hydrophobic chains and fluorine (ethyl, diethyl, pentyl and trifluoromethyl) to the benzimidazole moiety like **4a**, **4g**, **4i**, **4l** showed very less docking scores than with the aromatic substituents sulphonic acid, -NO_2 and –OCH_3 group of the compounds.

The docking results of the protein DNA gyrase subunit B of *S. aureus* (4P8O) reveals that the co-crystal ligand 883 showed greater interaction compared with the all the docked compounds with docking score -6.938. In 883 ligand interactions, the benzimidazole pharmacophore does not show any interaction with the protein active site. But the urea carbonyl group of 883 ligand showed interactions with water residue 442 and it makes a bond with amino acid ASN 44. In the case of compounds library, even though benzimidazole pharmacophore making interactions with the protein active site amino acid residues ASN 44 and GLU 58 (except **4c**, **4e**, **4k** and **4l**) showed less docking scores compared with 883 co-crystal. Like co-crystal, the compounds also (except **4e**, **4g** and **4h**) have similar interactions with water residues 442 and 471 and

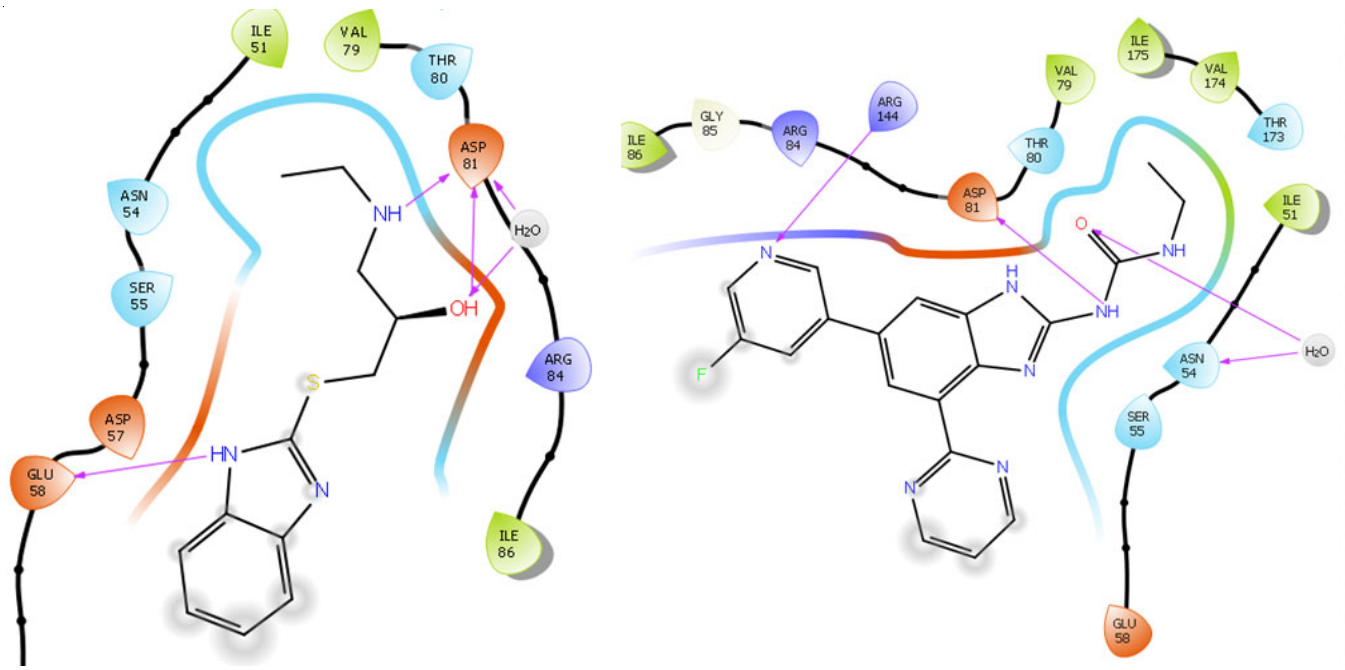

Compound **4a** (D.Score -6.155), H-bonding with GLU 58, ASP 81 and water residue 471 with ASP 81

Co-crystal ligand 883 (D.Score -6.938), H-bonding with ASP 81, ARG 144 and water residue 442 with ASN 54

Fig. 2. 2D interactions of compound **4a** and 883 ligand at the active site of protein *S. aureus* DNA Gyrase B (4P8O)

with ASN 44 and ASP 81 amino acid residues, respectively. The **4a** compound showed a high docking score -6.155 amongst docked compounds represented in Fig. 2.

The antifungal effectiveness of the synthesized compounds was estimated by their docking score and interactions with amino acid residues of the lanosterol 14α-demethylase proteins 5V5Z and 3LD6, the results are shown in Table-2.

Docking results of compounds with protein lanosterol 14α-demethylase of *Candida albicans* (5V5Z) revealed that the co-crystal ligand Itraconazole showed -9.629 docking score, one H-bond interaction with GLN 66 and Hydrophobic interactions with TYR 118, HIE 377 and HEM 601. But the compound **4l** showed excellent docking score -10.322, the 2º amine of benzimidazole ring, 2º amine of substitution and 2º alcohol makes three H-bond interactions with SER 378, SER 507, MET 508 amino acid residues and benzene ring of benzimidazole makes hydrophobic interaction with amino acid TYR 118 of the protein. The rest of the compounds also showed good to moderate interactions with protein, the pentyl substituted compound **4i** showed less docking score -6.610 among the all compounds shown in Fig. 3.

In the virtual screening of compounds with protein human LAD-CYP 51 (3LD6), the co-crystal ligand ketoconazole (KKK) showed docking score -9.379 with only one H-bond interaction with ILE 379 and hydrophobic interactions with HIE 236, TRP 239 and HIS 489. From the docked compounds, the compounds **4l** and **4h** showed greater docking score -9.950 and -9.597 compared with KKK ligand of protein. The compound **4l** greater docking score due to H-bond interaction of 2º alcohol, 2º amine of substitution with ILE 379, The 2º amine of benzimidazole pharmacophore with MET 487 amino acid residue and benzene ring of benzimidazole hydrophobic interaction with PHE 234 at the active site of a protein. As like, the compound **4h** showed two H-bond interactions with amino acid residues HIS 489 and PRO 376 by 2º alcohol and NH of benzimidazole, respectively. The rest of the compounds also showed good to moderate interactions with protein, the pentyl substituted compound **4i** showed less docking score -6.595 among the all compounds shown in Fig. 4.

ADME prediction: The ADME prediction data from the Swiss ADME database (Table-3), all the compounds obeys Lipinski's rule of 5 without any violations. From the prediction data, the GI absorption is high for compounds except compound **4d** due to the presence of -SO_2OH substitution. All the compounds not having BBB permeation except the compounds **4g** and **4i** due to the presence of diethyl and pentyl group, their hydrophobicity (LogP) is more 2.83 and 2.96, respectively compared with other compounds. The skin permeability LogKp is high for the compound **4b** amongst all the compounds because it is having only hydrazine substitution, no other alkyl or aryl group substitutions.

Antimicrobial activity: The synthesized compounds screened aginst for their antimicrobial activity aginst *E. coli*, *S. aureus* and *C. albicans*, the results were showed in Table-4.

The antimicrobial screening results against Gram-negative *E. coli* reveals that the compounds **4c**, **4e** and **4f** were effectively inhibited *E. coli* with their excellent MIC values at concen-

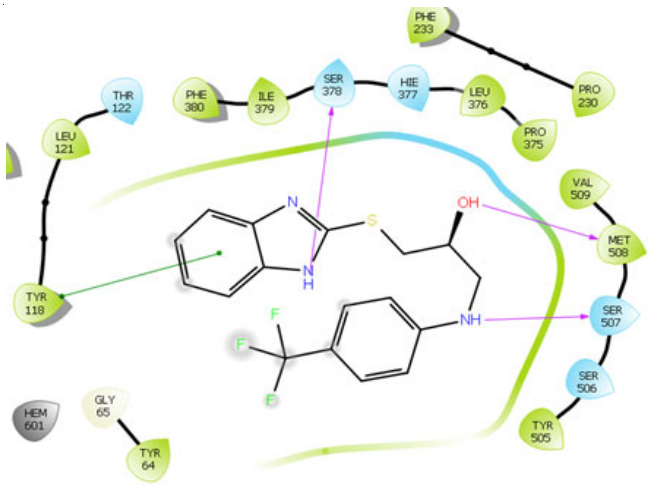

Compound **4l** (D.Score -10.322), H-bonding with SER 378, SER 507, MET 508 and Hydrophobic interaction with TYR 118

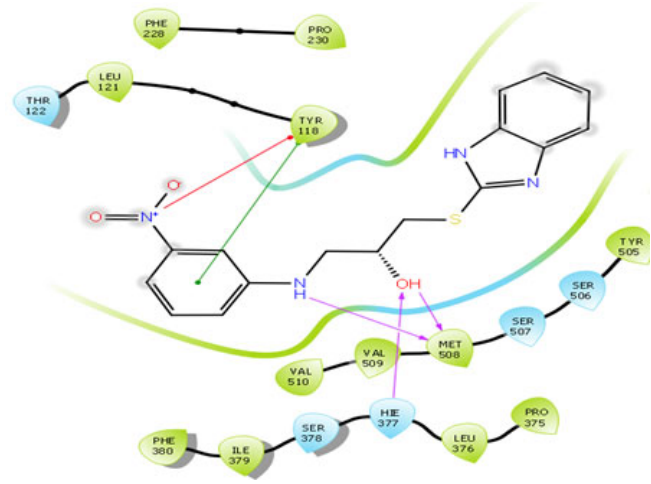

Compound **4j** (D.Score -9.155), H-bonding with HIE 377, MET 508 and Hydrophobic interaction with TYR 118

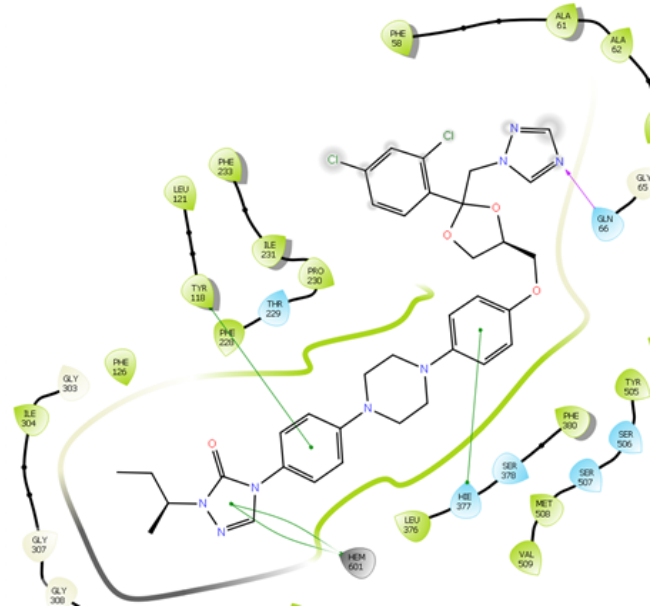

Itraconazole 1YN (D.Score -9.629), H-bonding with GLN 66 and Hydrophobic interaction with TYR 118, HIE 377 and HEM 601

Fig. 3. 2D Interactions of compound **4l**, **4J** and 1YN ligand with amino acid residues of protein CYP 51 from *Candida albicans* (5V5Z)

TABLE-2
DOCKING SCORE AND INTERACTIONS OF COMPOUNDS WITH LANOSTEROL 14α-DEMETHYLASE

Compound code	CYP 51 from *Candida albicans* (5V5Z)		Human LAD - CYP 51 (3LD6)	
	Docking score	Interactions	Docking score	Interactions
4a	-8.084	HIE 377, SER 378, SER 507, MET 508 and TYR 118 (Hydrophobic)	-7.635	ILE 379, MET 380
4b	-8.669	HIE 377, SER 378, TYR 505, SER 507 and TYR 118 (Hydrohobic)	-7.344	PRO 376, ILE 379,
4c	-8.526	HIE 377 (Hydrophobic), SER 378, MET 508 and TYR 132 (Hydrophobic)	-8.578	PRO 376, MET 487, HIS 489
4d	-8.794	HIE 377, SER 378, TYR 505	-8.944	TYR 131, PRO 376, ILE 379
4e	-8.546	SER 507, MET 508, TYR 132 (Hydrophobic), HEM 601 (Hydrophobic)	-7.948	PRO 376, MET 378
4f	-8.231	SER 378, MET 508 and TYR 118 (Hydrophobic)	-8.011	PRO 376, MET 378
4g	-7.899	TYR 505, MET 508	-7.656	TYR 131, ILE 379
4h	-8.582	MET 508 (H-Bond), HIE 377, PHE 380 and HEM 601 (Hydrophobic)	-9.597	PRO 376, HIS 489
4i	-6.610	HIE 377, SER 378, TYR 505, MET 508 and TYR 64 (Hydrophobic)	-6.595	TYR 131, ILE 379
4j	-9.155	HIE 377, MET 508 and TYR 118 (Hydrophobic)	-9.091	MET 487, HIS 489
4k	-8.413	SER 378, TYR 505, SER 507, MET 508 and TYR 64 (Hydrophobic)	-8.191	PRO 376, MET 378
4l	-10.322	SER 378, SER 507, MET 508 and TYR 118 (Hydrophobic)	-9.950	ILE 379, MET 487, PHE 284 (Hydrophobic)
Co-crystal	-9.629 (Itraconazole)	GLN 66 (H-bond), TYR 118, HIE 377 and HEM 601 (Hydrophobic)	-9.379 (Ketoconazole)	ILE 379 (H-Bond), HIE 236, TRP 239, HIS 489 (Hydrophobic)

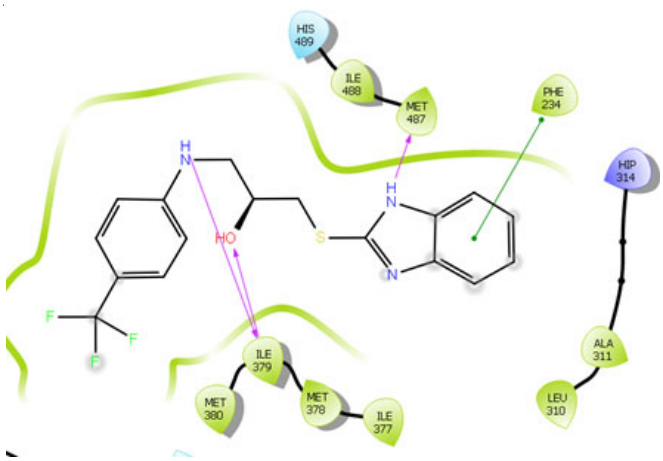

Compound **4l** (D.Score -9.950), H-bonding with ILE 379, MET 487 and Hydrophobic interaction with PHE 234

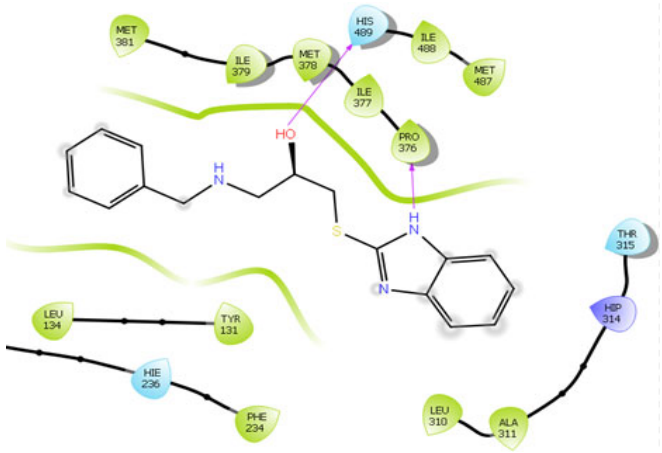

Compound **4h** (D.Score -9.597), H-bonding with PRO 376, HIS 489

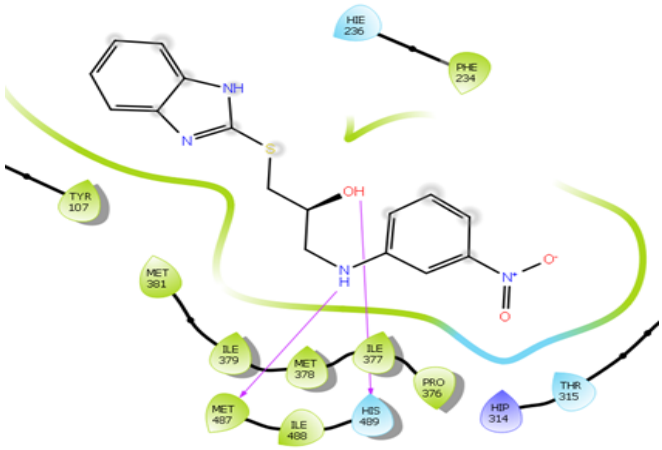

Compound **4j** (D.Score -9.091), H-bonding with MET 487, HIS 489

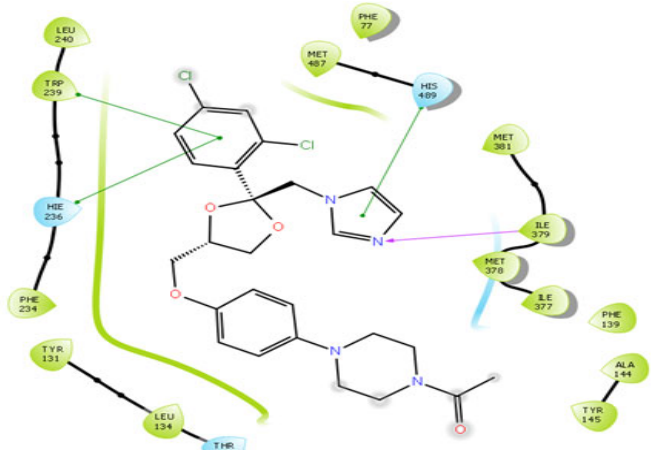

Ketoconazole KKK (D.Score -9.379), H-bonding with ILE 379 and Hydrophobic interaction with HIS 236, TRP 239, HIS 489

Fig. 4. 2D interactions of compound **4l**, **4h**, **4j** and KKK ligand with amino acid residues of protein human LAD-CYP 51 (3LD6)

TABLE-3
ADME PROPERTIES OF COMPOUNDS BY SWISS ADME *in silico* SOFTWARE

Compd. code	m.w.	Log P	Molar refractivity	TPSA	HBA	HBD	RB	GI absorption & BBB permeant	Log Kp (cm/s)	Logs	CYP inhibition					Lead likeness	SA
											1A2	2C19	2C9	2D6	3A4		
4a	251.35	2.37	71.01	86.24	3	3	6	High & No	-6.83	-2.29	No	No	No	No	No	Yes	2.86
4b	238.31	1.26	64.1	112.26	4	4	5	High & No	-7.53	-1.6	No	No	No	No	No	No	2.9
4c	314.41	2.14	90.22	98.27	3	4	7	High & No	-5.58	-4.17	Yes	Yes	Yes	Yes	Yes	No	3.51
4d	379.45	0.72	97.28	148.99	5	4	7	Low & No	-7.1	-3.52	Yes	No	No	No	No	No	3.33
4e	314.41	2.09	91.82	112.26	2	4	6	High & No	-6.29	-3.61	Yes	Yes	Yes	Yes	Yes	Yes	3.16
4f	299.39	2.41	87.42	86.24	2	3	6	High & No	-5.72	-3.96	Yes	Yes	Yes	Yes	Yes	Yes	3.02
4g	279.4	2.83	80.71	77.45	3	2	7	High & Yes	-6.4	-2.88	Yes	No	No	Yes	No	Yes	3.07
4h	313.42	2.6	90.69	86.24	3	3	7	High & No	-6.24	-3.58	No	Yes	Yes	Yes	Yes	Yes	2.91
4i	293.43	2.96	85.43	86.24	3	3	8	High & Yes	-5.98	-3.34	No	No	No	Yes	No	No	3.39
4j	344.39	1.96	96.24	132.06	4	3	7	High & No	-6.11	-4	Yes	No	Yes	Yes	No	Yes	3.43
4k	329.42	2.74	93.91	95.47	3	3	7	High & No	-5.92	-4.03	Yes	Yes	Yes	Yes	Yes	Yes	3.08
4l	367.39	2.52	92.42	86.24	5	3	7	High & No	-5.5	-4.8	Yes	Yes	Yes	Yes	Yes	No	3.08

TPSA = Topological polar surface area; HBA = Hydrogen bond acceptors; HBD = Hydrogen bond donors; RB = Rotational bonds; SA = Synthetic accessibility.

TABLE-4
ANTIMICROBIAL ACTIVITY OF SYNTHESIZED THIOBENZIMIDAZOLE DERIVATIVES (**4a-l**)

Compound code	Minimum inhibitory concentration (μg/mL)		
	Escherichia coli	*Staphylococcus aureus*	*Candida albicans*
4a	12.5	6.25	6.25
4b	12.5	12.5	3.12
4c	3.12	12.5	1.6
4d	12.5	12.5	1.6
4e	3.12	6.25	6.25
4f	6.25	12.5	6.25
4g	12.5	25	12.5
4h	25	25	0.8
4i	50	50	25
4j	12.5	3.12	0.8
4k	25	25	3.12
4l	25	3.12	0.4
Ciprofloxacin	12.5	6.25	–
Fluconazole	–	–	1.6

trations 3.12, 3.12 and 6.25 μg/mL than the ciprofloxacin standard MIC 12.5 μg/mL. and the compounds **4a**, **4b**, **4d**, **4g** and **4j** exhibited MIC value 12.5 μg/mL as that of ciprofloxacin. The remaining compounds except **4i** (50 μg/mL) showed antibacterial activity towards *E. coli* at 25 μg/mL. The compounds **4c**, **4e** and **4f** were having 2º amine linking with alkyl and aryl benzene without any substitution from the reaction of aromatic amines of phenyl hydrazine, *o*-phenylene diamine and aniline, respectively. It indicates that the aliphatic amine containing compounds except **4i** showed good inhibition. Then in the substituted aromatic amine compounds with sulphonic acid (**4d**), nitro (**4j**) showed better inhibition than the substitutions with benzylamine (**4h**), methoxy (**4k**) and trifluoromethyl (**4l**) substitutent.

The screening against *S. aureus* reveals, the compounds **4j**, **4l** showed excellent inhibition at MIC value 3.12 μg/mL compared with standard ciprofloxacin MIC 6.25 μg/mL. The compounds **4a**, **4e** also showed good activity MIC at 6.25 μg/mL. The compounds **4b**, **4c**, **4d**, **4f** showed inhibition MIC at 12.5 μg/mL and the remaining compounds except **4i** (50 μg/mL) exhibited activity MIC at 25 μg/mL. The nitro and trifluoromethyl substituted **4j** and **4l** showed excellent activity than the other amine substitutions of aromatic and aliphatic. In case of antifungal screening, **4l**, **4h** and **4j** exhibited excellent inhibition against *C. albicans* MIC at 0.4, 0.8 and 0.8 μg/mL, respectively when compared with standard fluconazole MIC at 1.6 μg/mL. **4c** and **4d** compounds showed activity at MIC 1.6 μg/mL, **4b** and **4k** showed activity MIC at 3.12 μg/mL, the compounds **4a**, **4e** and 4f exhibited activity at 6.25 μg/mL, **4g** and **4i** showed activity at 12.5 and 25 μg/mL, respectively. Among all the synthesized compounds, trifluoromethyl substituted benzimidazole represented excellent activity at MIC 0.4 μg/mL. From these antimicrobial screening results, the pentyl substitution compound **4i** represented the least activity. The docking studies also reveal that the compounds having more docking scores with lanosterol 14α-demethylase when compared with DNA gyrase subunit B proteins. Similarly in the screening results the compounds have more fungal inhibition compared to bacteria.

Conclusion

The proposed scheme led to the expected novel potent benzimidazole derivatives. *in silico* ADME of compounds reveals that no violations as per Lipinski's rule and the properties skin permeability, GI absorption, BBB permeation, CYP inhibition, leadlikeness and synthetic accessibility, *etc*. ultimately helps in the *in vivo* studies and clinical phase studies of such compounds. The compounds showed excellent docking scores and interactions with lanosterol 14α-demethylase as standard co-crystal ligand of proteins compared with DNA gyrase subunit B proteins. These docking studies against DNA Gyrsea subunit B and lanosterol 14α-demethylase proteins gave a good platform for further *in vitro* antimicrobial screening. In antimicrobial *in vitro* studies also its clear that the compounds showed excellent fungal activity than bacterial activity compared with their standards. The compound **4l** trifluoromethyl substituted benzimidazole derivative exhibited excellent antifungal activity at MIC 0.4 μg/mL against *C. albicans* and also excellent docking score towards lanosterol 14α-demethylase 5V5Z protein -10.322 (standard co-crystal Itraconazole 1YN docking score -9.629) and with 3LD6 protein -9.950 (standard co-crystal Ketoconazole KKK docking score -9.379).

The compounds **4c** and **4e** exhibited antibacterial inhibition at MIC 3.12 µg/mL against *E. coli* and also showed excellent docking scores against DNA gyrase subunit B 5L3J protein -7.096 and -6.935, respectively (standard co-crystal 6G9 docking score -6.423).

ACKNOWLEDGEMENTS

The authors are thankful to DST-SERB and DST-FIST Laboratory, Raghavendra Institute of Pharmaceutical Education and Research (RIPER), Anantapur-515721, India for providing the facility of Schrodinger Glide Software for molecular modeling work.

CONFLICT OF INTEREST

The authors declare that there is no conflict of interests regarding the publication of this article.

REFERENCES

1. N. Jackson, L. Czaplewski and L.J.V. Piddock, *J. Antimicrob. Chemother.*, **73**, 1452 (2018); https://doi.org/10.1093/jac/dky019
2. Salahuddin, M. Shaharyar and A. Mazumder, *Arab. J. Chem.*, **10(Supl. 1)**, S157 (2017); https://doi.org/10.1016/j.arabjc.2012.07.017
3. A.T. Mavrova, K.K. Anichina, D.I. Vuchev, J.A. Tsenov, P.S. Denkova, M.S. Kondeva and M.K. Micheva, *Eur. J. Med. Chem.*, **41**, 1412 (2006); https://doi.org/10.1016/j.ejmech.2006.07.005
4. F. Hobrecker, *Ber.*, **5**, 920 (1872); https://doi.org/10.1002/cber.18720050295
5. M. Tuncbilek, T. Kiper and N. Altanlar, *Eur. J. Med. Chem.*, **44**, 1024 (2009); https://doi.org/10.1016/j.ejmech.2008.06.026
6. A.K. Tewari and A. Mishra, *Indian J. Chem.*, **45B**, 489 (2006).
7. R.D. Haugwitz, R.G. Angel, G.A. Jacobs, B.V. Maurer, V.L. Narayanan, L.R. Cruthers and J. Szanto, *J. Med. Chem.*, **25**, 969 (1982); https://doi.org/10.1021/jm00350a017
8. M. Gjorgjieva, T. Tomasic, M. Barancokova, S. Katsamakas, J. Ilas, P. Tammela, L.P. Masic and D. Kikelj, *J. Med. Chem.*, **59**, 8941 (2016); https://doi.org/10.1021/acs.jmedchem.6b00864
9. A.-L. Grillot, A.L. Tiran, D. Shannon, E. Krueger, Y. Liao, H. O'Dowd, Q. Tang, S. Ronkin, T. Wang, N. Waal, P. Li, D. Lauffer, E. Sizensky, J. Tanoury, E. Perola, T.H. Grossman, T. Doyle, B. Hanzelka, S. Jones, V. Dixit, N. Ewing, S. Liao, B. Boucher, M. Jacobs, Y. Bennani and P.S. Charifson, *J. Med. Chem.*, **57**, 8792 (2014); https://doi.org/10.1021/jm500563g
10. N. Strushkevich, S.A. Usanov and H.-W. Park, *J. Mol. Biol.*, **397**, 1067 (2010); https://doi.org/10.1016/j.jmb.2010.01.075
11. M.V. Keniya, M. Sabherwal, R.K. Wilson, M.A. Woods, A.A. Sagatova and D.A. Joel, *Antimicrob. Agents Chemother.*, **62**, e01134 (2018); https://doi.org/10.1128/AAC.01134-18
12. A. Daina, O. Michielin and V. Zoete, *Sci. Rep.*, **7**, 42717 (2017); https://doi.org/10.1038/srep42717
13. A. Daina, O. Michielin and V. Zoete, *J. Chem. Inf. Model.*, **54**, 3284 (2014); https://doi.org/10.1021/ci500467k
14. A. Daina and V. Zoete, *ChemMedChem*, **11**, 1117 (2016); https://doi.org/10.1002/cmdc.201600182
15. R. Schwalve, L.S. Moore and A.V. Goodwin, Antimicrobial Susceptibility Testing Protocols, CRC Press (2007).
16. H.D. Isenberg and L.S. Garcia, Clinical Microbiology Procedures Handbook, American Society for Microbiology, ASM Press Washington, DC, Vol 1 (2007).